10.1071/ES24002
Journal of Southern Hemisphere Earth Systems Science

Supplementary Material

Recent trends in extratropical lows and their rainfall over Australia

Acacia Pepler[A,*]

[A]Bureau of Meteorology, Sydney, NSW, Australia

*Correspondence to: Email: acacia.pepler@bom.gov.au

Supplementary Tables

Table S1. Linear trends (days per decade) in the number of days with surface, 500 hPa and deep lows over southern Australia during May–October and November–April for 1979–2023 (or 2014 in the case of CMIP6 models).

	May–October			November–April		
Model	**Surface**	**500 hPa**	**Deep**	**Surface**	**500 hPa**	**Deep**
ERA5	-0.65	-1.01	-0.61	-0.72	-0.49	-1.20
JRA55	-0.20	-0.59	-0.16	-0.50	0.04	-1.02
NCEP1	-0.21	0.24	0.68	-0.79	0.47	0.01
CMIP6 mean	-0.59	-0.68	-0.94	0.15	-0.13	-0.33
ACCESS-CM2	-0.83	**-2.03**	*-1.71*	1.09	0.07	0.02
ACCESS-ESM1-5	-0.76	-0.33	**-1.32**	0.79	0.49	*0.90*
CMCC-ESM2	-0.37	-0.47	-1.12	-0.42	-0.66	-1.50
CNRM-ESM2-1	-0.48	0.57	-0.35	-0.38	-0.41	-0.87
EC-Earth3	-0.63	-1.67	-1.27	*1.31*	0.23	0.34
MPI-ESM1-2-HR	*-1.59*	**-1.83**	*-1.83*	-0.40	-0.14	-0.25
MRI-ESM2-0	-0.52	-0.61	-1.03	-0.45	-0.31	-0.79
NorESM2-MM	0.47	0.93	1.13	-0.37	-0.27	-0.52

Bold indicates trends significant for $P < 0.05$, and italic for $P < 0.1$

Table S2. Linear trend (days per decade) in the May-October average number of days in southern Australia (33–43°S, 110–155°E) with a low pressure centre within a 10° radius over 1959–2023, for both ERA5 and JRA55.

	ERA5				JRA55			
Surface threshold	0.6	0.8	1	1.2	0.6	0.8	1	1.2
Upper threshold	5	6	8	10	5	6	8	10
Upper lows	-0.57	-0.47	-0.27	+0.12	0.05	0.22	**+0.85**	**+1.52**
Surface lows	**-1.62**	**-1.09**	*-0.71*	-0.19	**-1.84**	**-1.16**	-0.43	+0.05
Deep lows	-0.84	-0.70	-0.39	+0.20	-0.54	-0.29	+0.36	**+1.18**

Columns show a range of surface and 500-hPa intensity thresholds (with higher thresholds indicating more intense lows), and bold text indicates statistical significance for $P < 0.05$).

Table S3. Linear trend (days per decade) in the November-April average number of days in southern Australia (33–43°S, 110–155°E) with a low pressure centre within a 10° radius over 1959–60 to 2022–23, for both ERA5 and JRA55.

	ERA5				JRA55			
Surface threshold	0.6	0.8	1	1.2	0.6	0.8	1	1.2
Upper threshold	5	6	8	10	5	6	8	10
Upper lows	0.21	+0.13	-0.03	-0.14	0.33	0.23	+0.25	+0.29
Surface lows	**-0.78**	*-0.56*	-0.33	-0.07	**-1.76**	**-1.13**	**-0.49**	-0.09
Deep lows	-0.35	-0.24	-0.22	-0.05	-0.33	-0.29	-0.19	+0.32

Columns show a range of surface and 500-hPa intensity thresholds (with higher thresholds indicating more intense lows), and bold text indicates statistical significance for $P < 0.05$).

Supplementary Figures

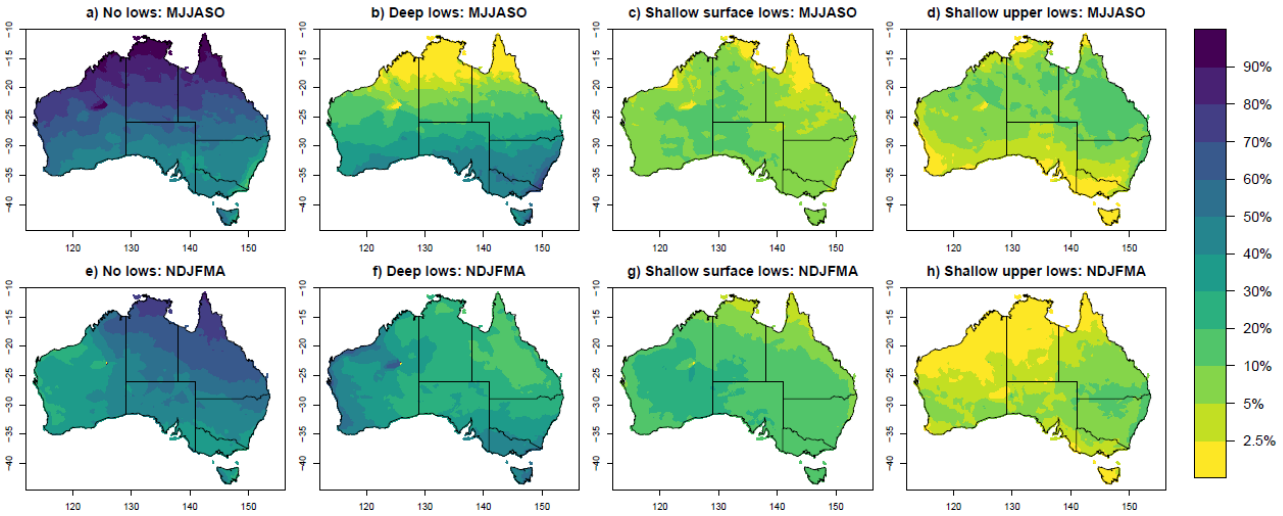

Figure S1. Proportion of May–October (top) and November–April (bottom) rain associated with different types of lows as detected from the ERA5 reanalysis during 1959–2023. Note non-linear colour scale for proportions below 10%.

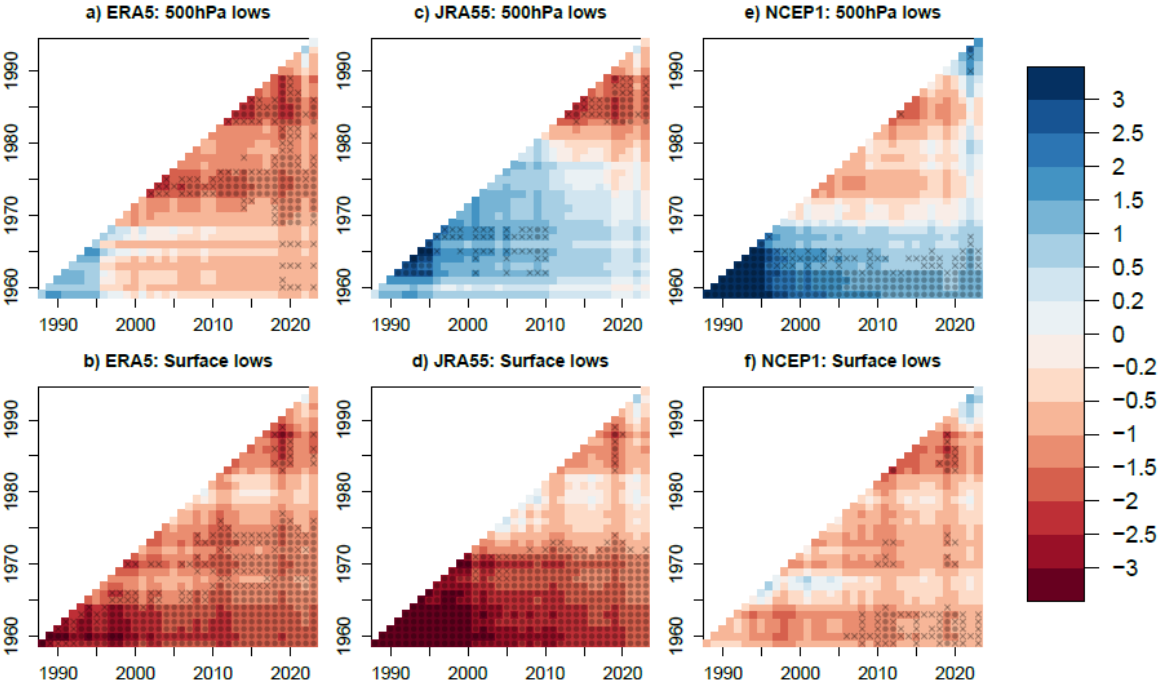

Figure S2. (left) Linear trend in the number of days influenced by a 500-hPa low (top) or surface low (bottom) across southern Australia in May–October over 1959–2023, in days per decade from the ERA5, JRA55 and NCEP1 re-analyses. Trends are shown for a range of periods between 1959 and 2023 of 30 years or longer, with solid circles indicating $P < 0.05$ and crosses $P < 0.1$.

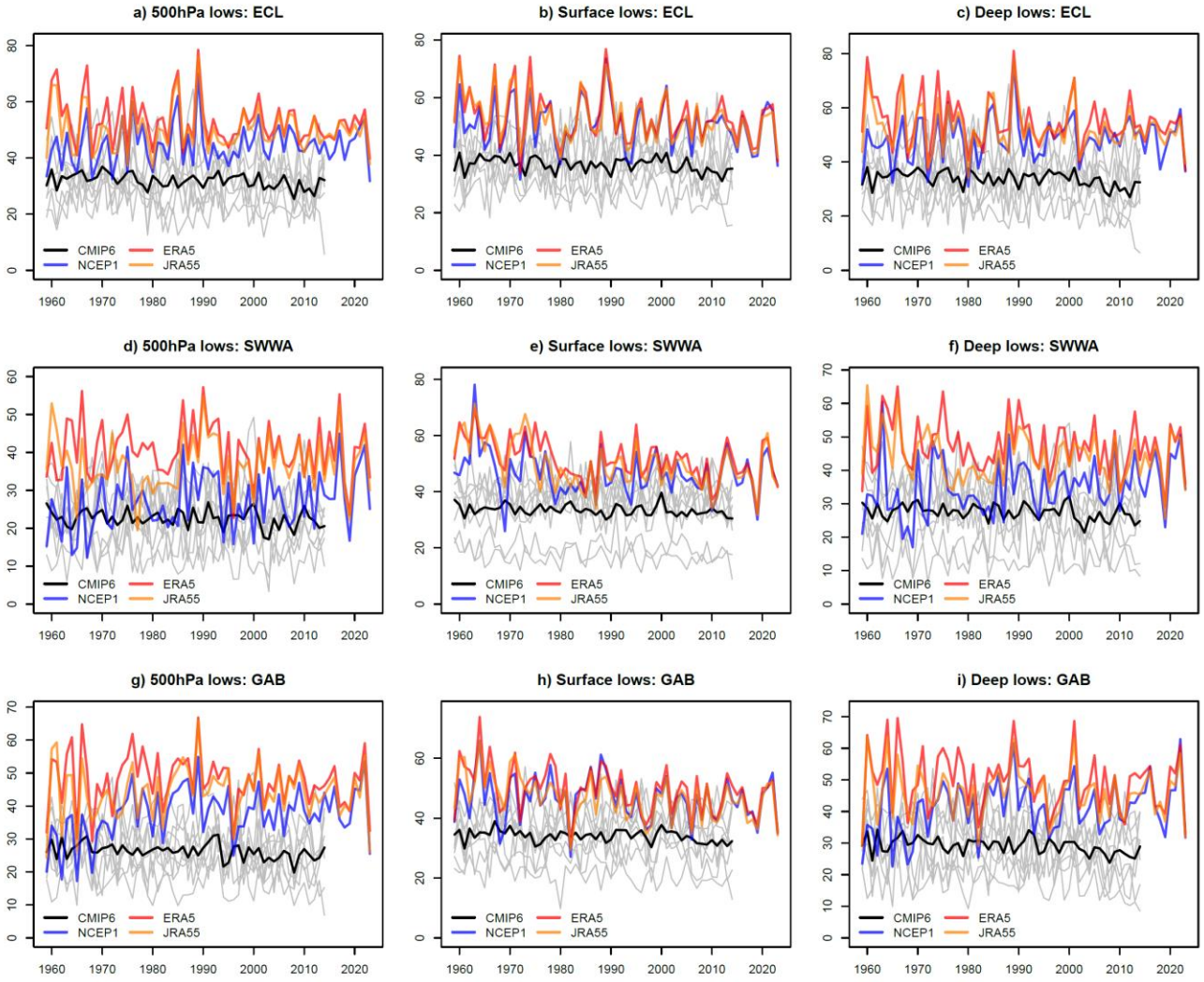

Figure S3. The percentage of days with a 500-hPa low (left), surface low (centre) or deep low (right) detected during 1959–2023 during May–October for three subregions of southern Australia from Figure 1: the East Coast Low (ECL) region in the Tasman Sea, south-western Western Australia (SWWA) and the Great Australian Bight (GAB). Coloured lines indicate 3 re-analyses and grey lines the 8 CMIP6 models, with black indicating the CMIP6 ensemble mean.

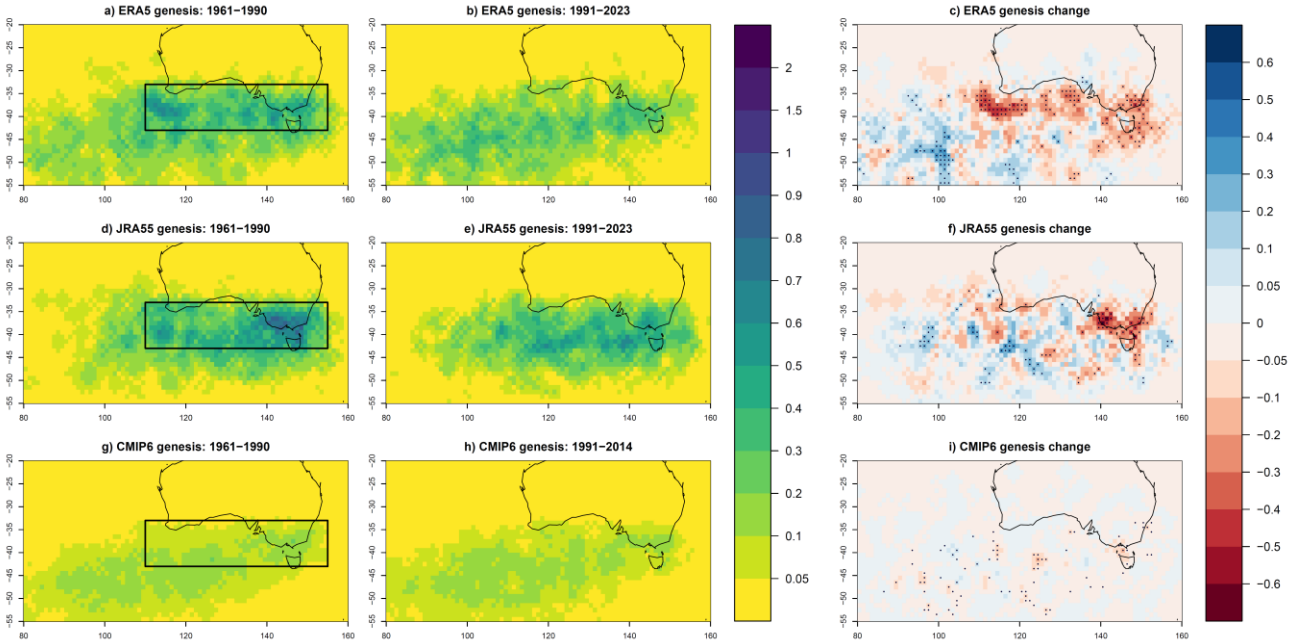

Figure S4. As in Figure 5, but for cyclogenesis of 500-hPa lows during May–October.

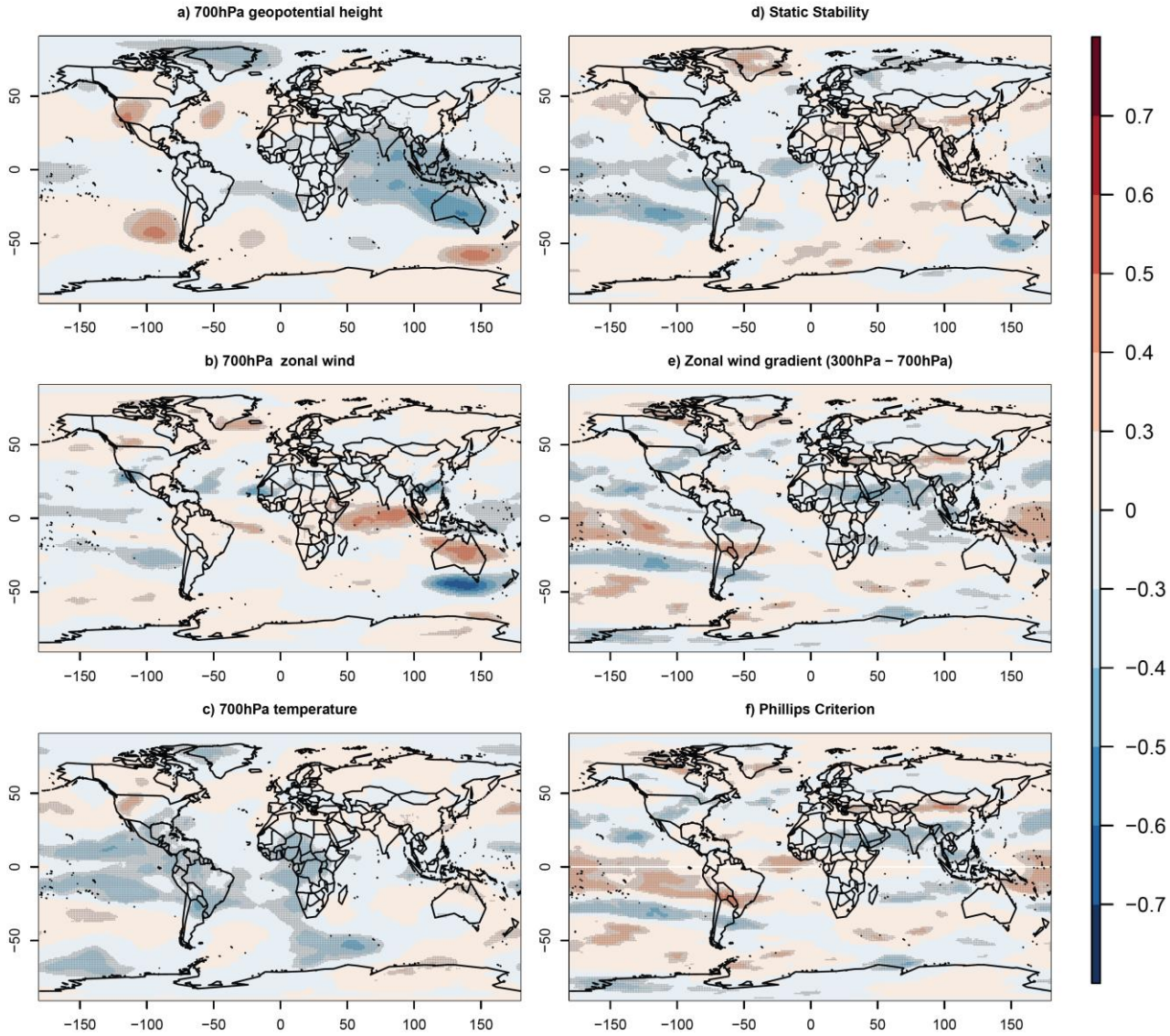

Figure S5. Correlations between detrended May-October counts of cyclone centres identified near southern Australia in ERA5 (33–43°S, 110–155°E) and six seasonal mean climate variables at each grid point over the same period 1959–2023, where dots indicate correlations that are statistically significant for $P < 0.05$. (a) 700-hPa geopotential height, (b) 700-hPa zonal wind; (c) 700-hPa air temperature, (d) Static stability, calculated following Frederiksen *et al*. (2016); (e) The difference between zonal wind at 300 and 700 hPa; (f) the Phillips Criterion, a measure of baroclinicity which incorporates both (d) and (e), following Frederiksen *et al*. (2016).

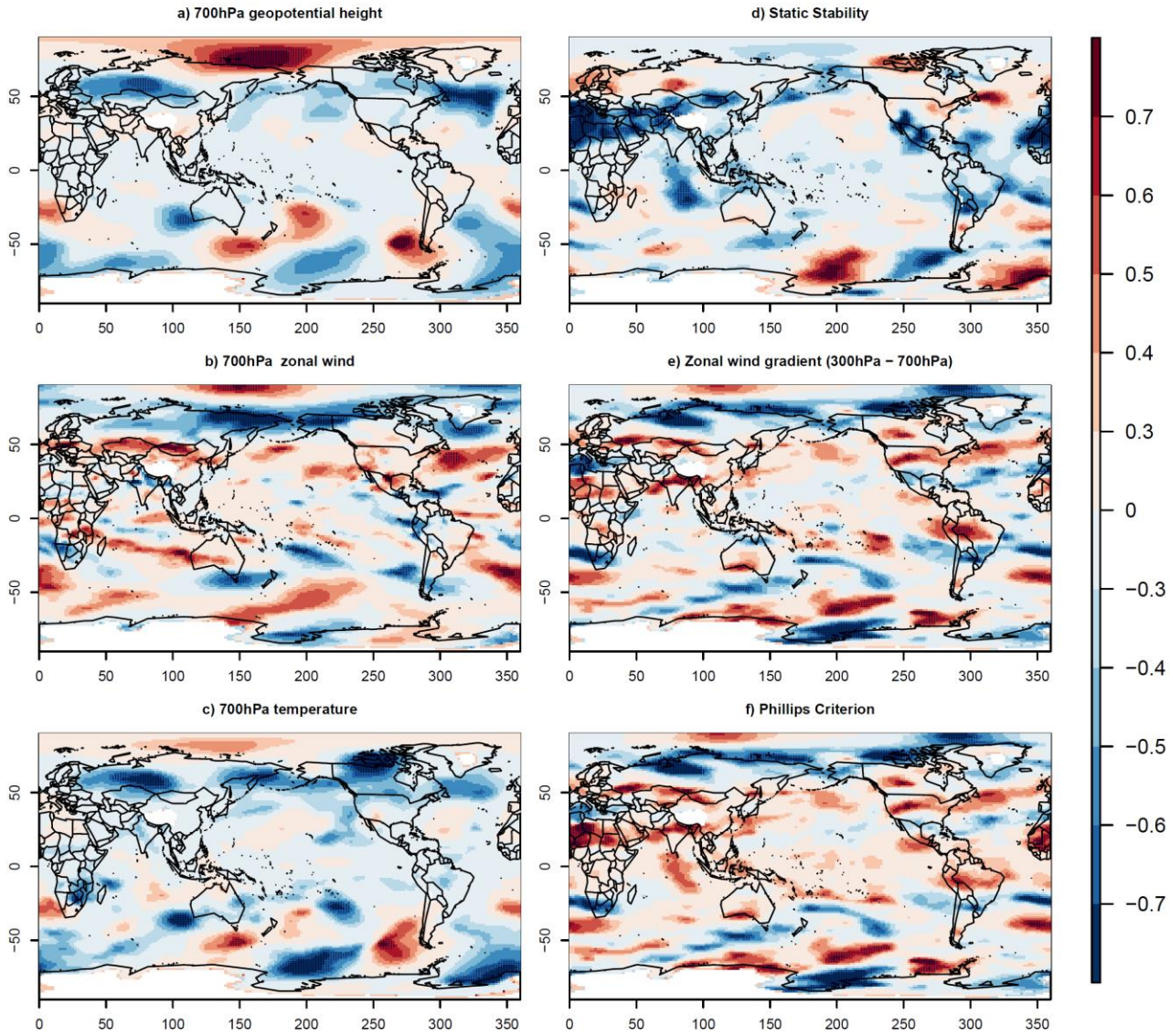

Figure S6. Correlations across the 10-member ACCESS-ESM1.5 historical ensemble between May-October linear trends in the number of cyclone centres identified near southern Australia (33–43°S, 110-155°E) and the linear trend in six seasonal mean climate variables at each grid point over the same period 1960–2014, where dots indicate correlations that are statistically significant for $P < 0.05$ (i.e. $r > 0.576$). (a) 700-hPa geopotential height, (b) 700-hPa zonal wind; (c) 700-hPa air temperature, (d) static stability, calculated following Frederiksen et al. (2016); (e) The difference between zonal wind at 300 and 700 hPa; (f) the Phillips Criterion, a measure of baroclinicity which incorporates both (d) and (e), following Frederiksen et al. (2016).

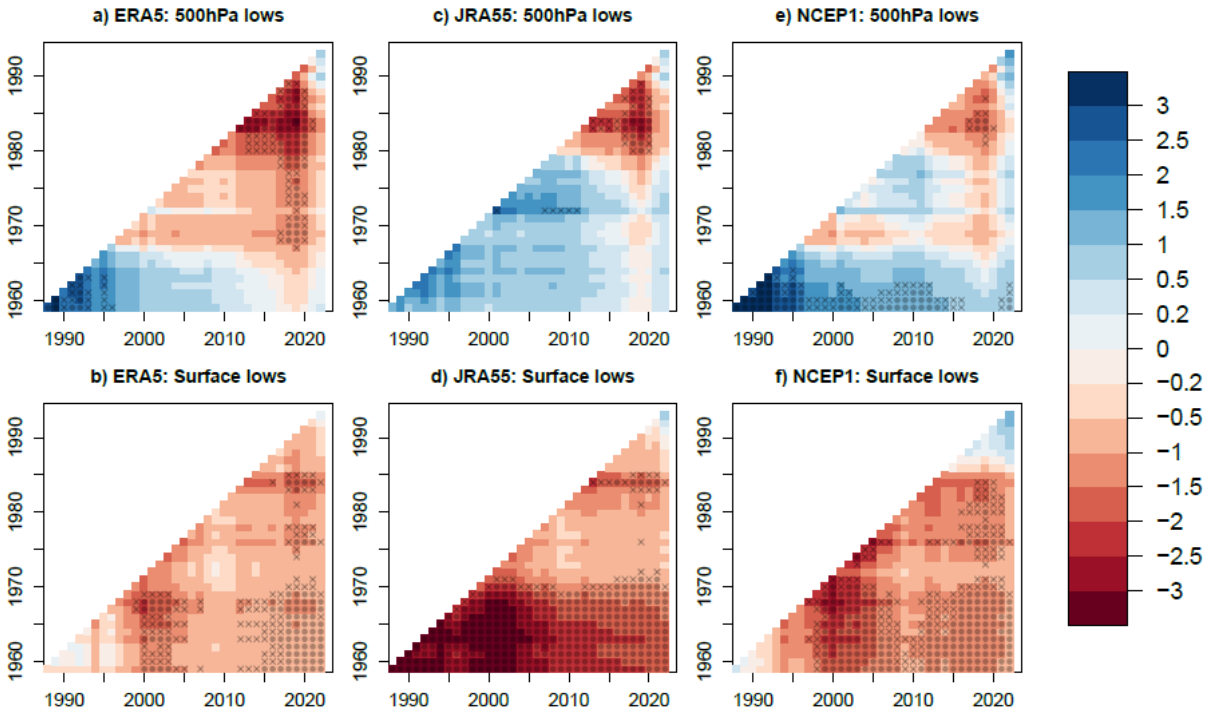

Figure S7. (left) Linear trend in the number of days influenced by a 500-hPa low (top) or surface low (bottom) across southern Australia in November–April over 1959–2023, in days per decade from the ERA5, JRA55 and NCEP1 re-analyses. Trends are shown for a range of periods between 1959 and 2023 of 30 years or longer, with solid circles indicating $P < 0.05$ and crosses $P < 0.1$.

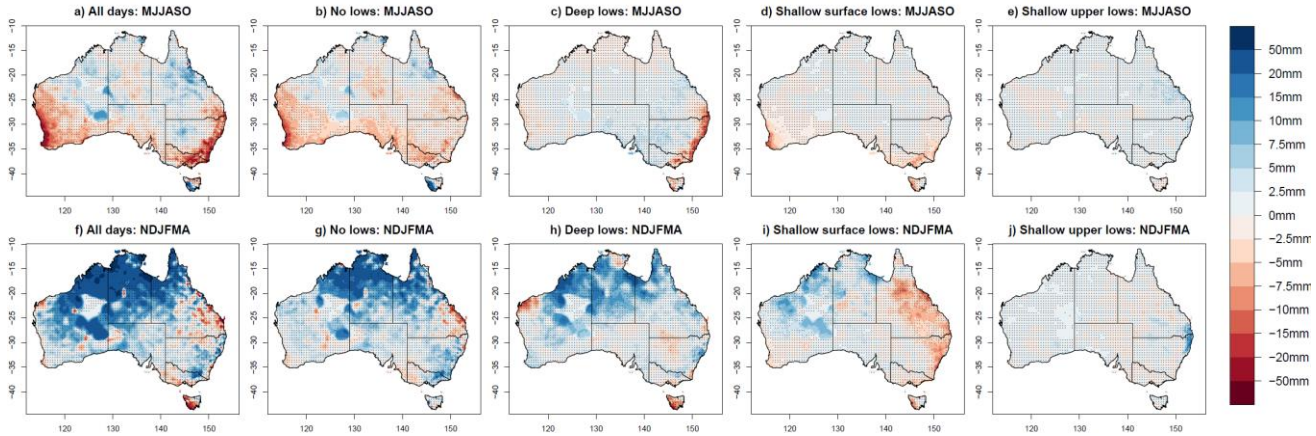

Figure S8. (left) Linear trend in total May–October (top) and November–April (bottom) rainfall over 1959–2023, in millimetres per decade. Also shown are linear trends in the total seasonal rainfall accumulated across days with no low, a deep low, a shallow surface low, or a shallow upper low in JRA55.

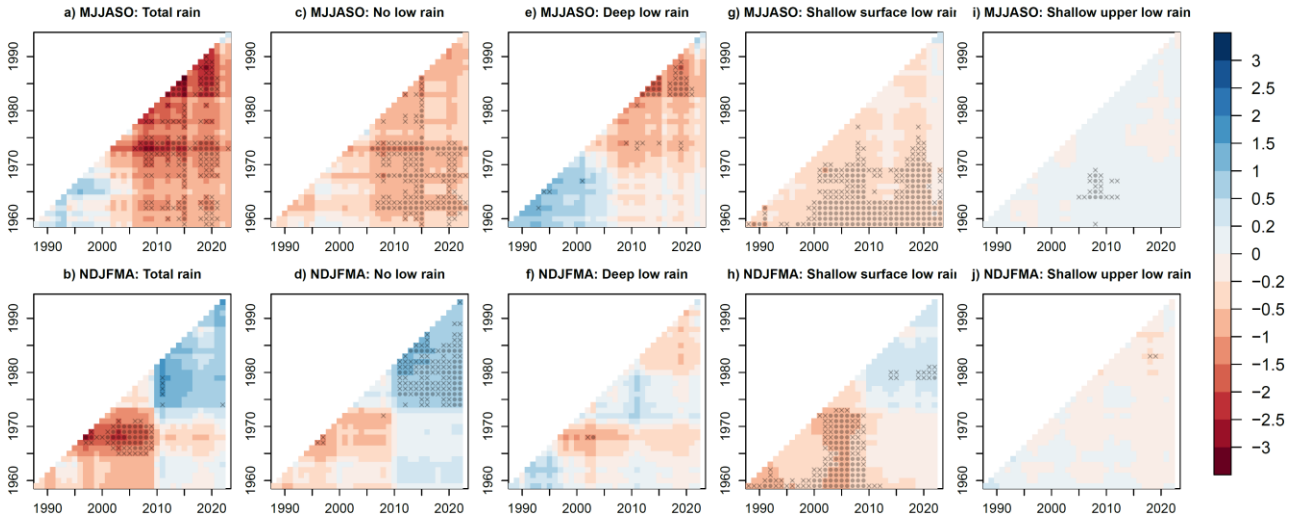

Figure S9. Linear trend (mm year^{-1}) in total seasonal rainfall in Southern Australia (left) during MJJASO (top) and NDJFMA (bottom), as well as the trend in rainfall linked to three categories of low and days with no lows using the JRA55 reanalysis. Trends are shown for a range of periods between 1959 and 2023 of 30 years or longer, with solid circles indicating $P < 0.05$ and crosses $P < 0.1$.

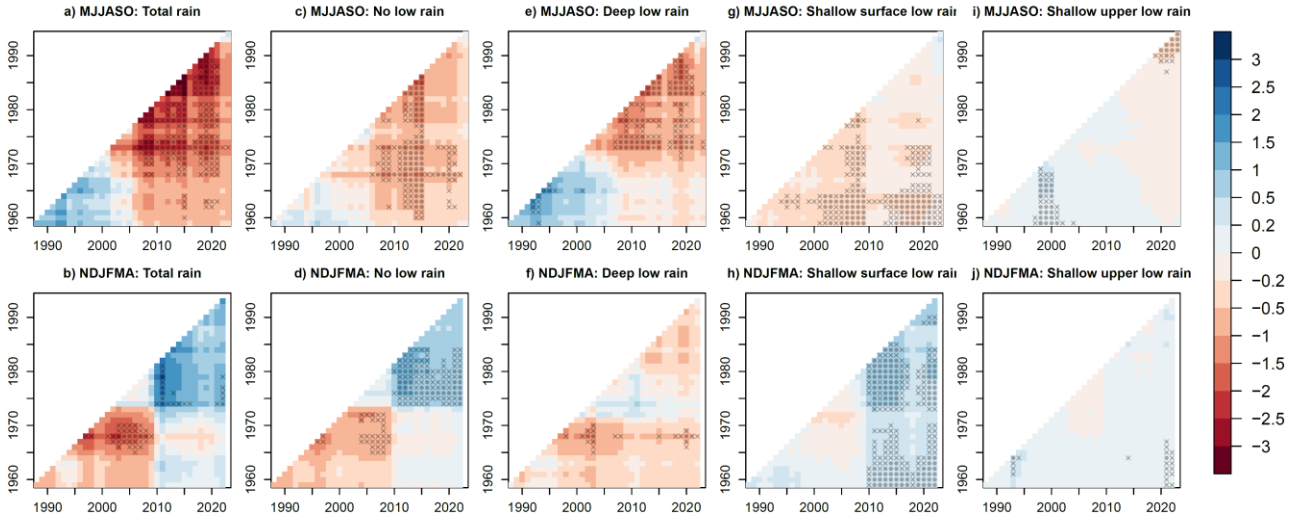

Figure S10. As in Figure S9, but for SEA using ERA5.

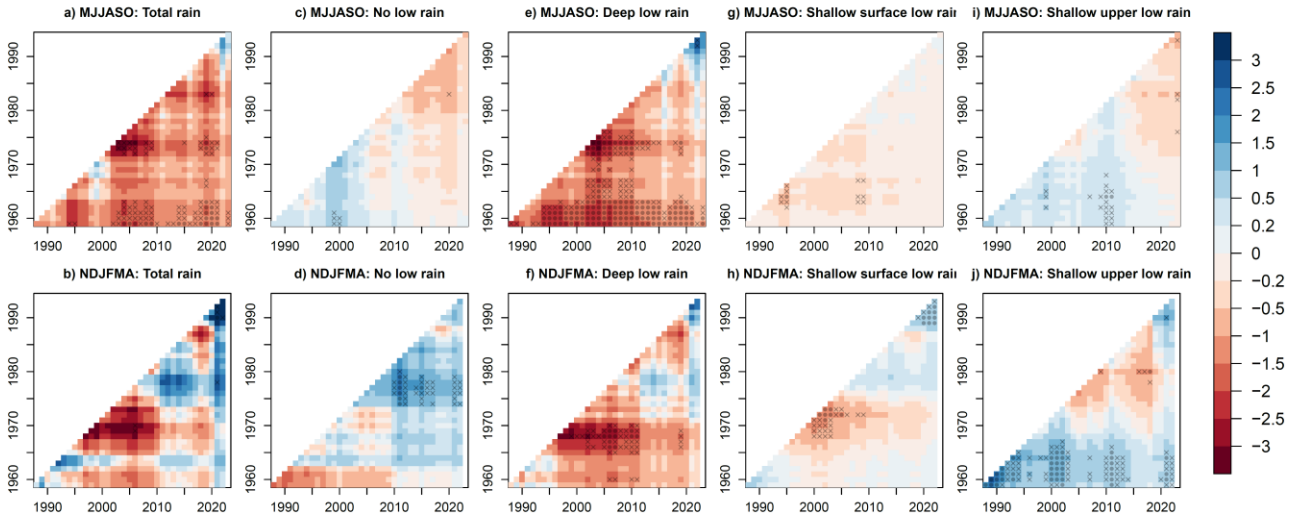

Figure S11. As in Figure S9, but for the ESB using ERA5.

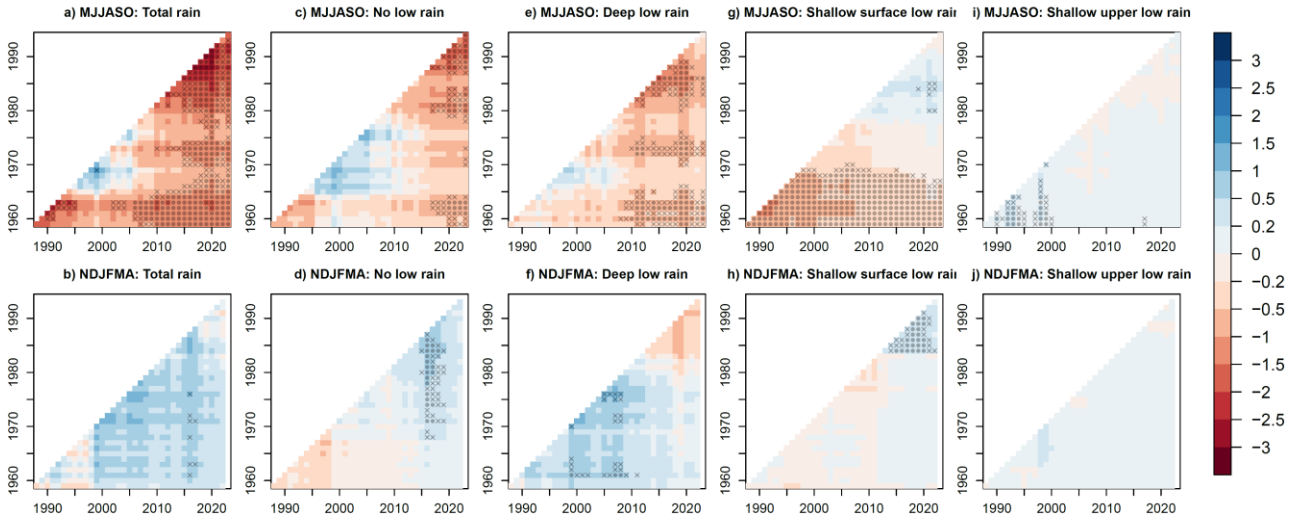

Figure S12. As in Figure S9, but for SWWA using ERA5.

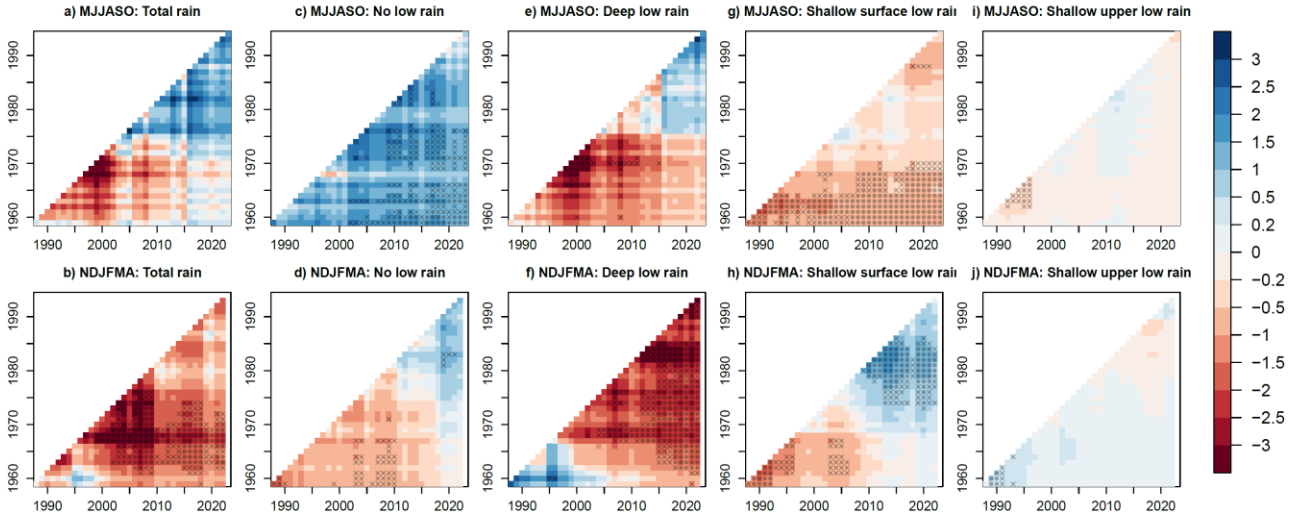

Figure S13. As in Figure S9, but for TAS using ERA5.

Reference

Frederiksen CS, Frederiksen JS, Sisson JM, Osbrough SL (2016) Trends and projections of Southern Hemisphere baroclinicity: the role of external forcing and impact on Australian rainfall. *Climate Dynamics* **48**(9–10), 3261–3282. doi:10.1007/s00382-016-3263-8